Water Research 135 (2018) 207–219

Contents lists available at ScienceDirect

Water Research

journal homepage: www.elsevier.com/locate/watres

Microbial community characterization of ozone-biofiltration systems in drinking water and potable reuse applications

Daniel Gerrity [a, *], Mayara Arnold [a], Eric Dickenson [b], Duane Moser [c], Joshua D. Sackett [c, d], Eric C. Wert [b]

[a] Department of Civil and Environmental Engineering and Construction, University of Nevada, Las Vegas, Box 454015, 4505 S. Maryland Parkway, Las Vegas, NV 89154-4015, United States
[b] Applied Research and Development Center, Southern Nevada Water Authority, P.O. Box 99954, Las Vegas, NV 89193, United States
[c] Desert Research Institute, 755 E. Flamingo Rd. Las Vegas, NV 89119, United States
[d] School of Life Sciences, University of Nevada, Las Vegas, 4505 S. Maryland Parkway, Las Vegas, NV 89154-4015, United States

ARTICLE INFO

Article history:
Received 27 September 2017
Received in revised form
7 February 2018
Accepted 8 February 2018
Available online 13 February 2018

Keywords:
Ozone
Drinking water
Wastewater
Biofiltration
16S rRNA gene sequencing
Microbial community

ABSTRACT

Microbial community structure in the ozone-biofiltration systems of two drinking water and two wastewater treatment facilities was characterized using 16S rRNA gene sequencing. Collectively, these datasets enabled comparisons by facility, water type (drinking water, wastewater), pre-oxidation (ozonation, chlorination), media type (anthracite, activated carbon), media depth, and backwash dynamics. Proteobacteria was the most abundant phylum in drinking water filters, whereas Bacteroidetes, Chloroflexi, Firmicutes, and Planctomycetes were differentially abundant in wastewater filters. A positive correlation was observed between media depth and relative abundance of Cyanobacteria in drinking water filters, but there was only a slight increase in one alpha diversity metric with depth in the wastewater filters. Media type had a significant effect on beta but not alpha diversity in drinking water and wastewater filters. Pre-ozonation caused a significant decrease in alpha diversity in the wastewater filters, but the effect on beta diversity was not statistically significant. An evaluation of backwash dynamics resulted in two notable observations: (1) endosymbionts such as *Neochlamydia* and *Legionella* increased in relative abundance following backwashing and (2) nitrogen-fixing *Bradyrhizobium* dominated the microbial community in wastewater filters operated with infrequent backwashing. *Bradyrhizobium* is known to generate extracellular polymeric substances (EPS), which may adversely impact biofilter performance and effluent water quality. These findings have important implications for public health and the operation and resiliency of biofiltration systems.

1. Introduction

Microbial community structure can have a significant impact on water quality in engineered biological treatment systems. Conversely, operational variability in biological treatment systems may also impact the structure and function of the microbial community, particularly with respect to the removal of disinfection byproduct precursors (Liu et al., 2017) and other trace organic compounds (TOrCs) (Mikkelson et al., 2015; Vuono et al., 2015). Certain operational conditions may select for bacteria that are specifically adapted to biodegrade TOrCs through direct metabolic and/or co-metabolic processes (Fischer and Majewsky, 2014). For example, recent lab-scale studies have identified bacterial genera (*Rhodococcus* and *Mycobacterium*) capable of degrading *N*-nitrosodimethylamine (NDMA) (Sharp et al., 2010). Implementing operational changes that select for these bacteria would be advantageous for drinking water and potable reuse systems because NDMA is a potential carcinogen even at the low ng/L level. In addition to bulk and trace organics, characterization of microbial community structure may further our understanding of the public health risks associated with the accumulation of pathogenic bacteria within biological treatment systems.

The performance of engineered biofiltration systems can be impacted by several variables, including influent water quality, oxidative pretreatment, empty bed contact time (EBCT), and

* Corresponding author. Department of Civil and Environmental Engineering and Construction, University of Nevada, Las Vegas, Box 454015, 4505 S. Maryland Parkway, Las Vegas, NV 89154-4015, United States.
E-mail address: Daniel.Gerrity@unlv.edu (D. Gerrity).

https://doi.org/10.1016/j.watres.2018.02.023
0043-1354/

backwashing frequency. These variables generally affect the redox environment, which is known to influence the development and stability of the microbial community (Zhu et al., 2010; Velten et al., 2011; Jałowiecki et al., 2016). These factors have been studied to some degree in drinking water systems (Li et al., 2010; Liao et al., 2012, 2013a; 2013b) and managed aquifer recharge applications (Li et al., 2012, 2013). However, few studies have focused on advanced treatment trains in potable reuse applications (Li et al., 2017), and even fewer have directly compared biofiltration systems in drinking water versus wastewater matrices.

With recent advances in microbiology, molecular techniques now provide several powerful tools with which to explore these issues. For example, quantitative polymerase chain reaction (qPCR) can be used to target genes coding for enzymes linked to biodegradation of target contaminants (e.g., NDMA; Nelson and LaBelle, 2013), and quantitative stable isotope probing (qSIP) can be used to identify the specific microorganisms responsible for TOrC biodegradation (e.g., bisphenol A; Chandran, 2016). These tools facilitate the direct examination of microbial function and activity related to known genes and physiologies. However, they also risk missing contributions from uncharacterized genes, pathways, or members of the microbial community. A more comprehensive molecular examination can be achieved with (meta)genomics or transcriptomics, which utilize high throughput DNA and RNA sequencing technologies, respectively, and offer promising new angles to interrogate microbial community structure and function in the context of biotransformation (Johnson et al., 2015).

The use of next generation (or high-throughput) DNA sequencing (e.g., Illumina platform) is rapidly emerging as the default technique for cultivation-free assessment of microbial community structure in environmental science and engineering applications (Douterelo et al., 2014; Sinclair et al., 2015). This approach involves sequencing the 16S rRNA gene of Bacteria or Archaea or the 18S rRNA gene of eukaryotes (e.g., fungi and amoebae). These genes contain both highly conserved regions that allow for nonspecific amplification of target DNA and variable regions that allow for taxonomic differentiation and classification. In contrast with metagenomics and transcriptomics, targeting the 16S or 18S rRNA gene does not necessarily provide insight into microbial function, but the resulting data can be used to monitor shifts in microbial community structure caused by changes in environmental or operational conditions.

The current study integrates 16S rRNA gene sequencing datasets for ozone-biofiltration systems at two drinking water and two wastewater treatment facilities. These data were synthesized to (1) compare and contrast microbial communities in drinking water and wastewater filters and (2) evaluate the effects of filter design criteria and operational conditions on microbial community structure. The variables included oxidative pretreatment (ozonation and chlorination), media type [anthracite, granular activated carbon (GAC), and biological activated carbon (BAC)], media depth, and backwash dynamics. This information will facilitate a better understanding of the composition and resiliency of biofiltration systems and will provide a baseline for future studies aimed at elucidating links between bacterial taxa and biodegradation of target constituents.

2. Methodology

2.1. Study sites

Filter media samples were collected from two drinking water and two wastewater facilities, for which the corresponding treatment trains are illustrated in Fig. 1. Operational criteria, general water quality parameters, and sampling details are summarized in Table 1, and the 16S rRNA gene sequencing metadata are summarized in the Supplementary Information (SI) file in Tables S1 and S2. Because the filter media samples were originally collected for different studies, some procedures (e.g., DNA extraction and primer selection) differed slightly by sample location. For this reason, it was not advisable to aggregate sequencing data from all four facilities prior to data processing, reduction, and analysis. Instead, samples from drinking water treatment plant 1 (DWTP1), DWTP2, and reuse pilot 1 (RP1) were combined and analyzed simultaneously, while samples from RP2 were analyzed separately. In the following sections, presentation and discussion of the two datasets remain largely independent to minimize the potential for method bias to yield erroneous conclusions.

2.1.1. Drinking water treatment plant 1 (DWTP1)

The first study site (DWTP1) was a pilot-scale skid containing parallel GAC/sand and anthracite/sand filters fed with ozonated surface water (ozone/DOC = 0.8) following ferric chloride coagulation and flocculation. The filter columns had a diameter of 25 cm, and they contained 122 cm of either anthracite or GAC atop 30 cm of sand, although samples were only collected at a single depth of 25 cm. The GAC had been acclimated in a full-scale drinking water treatment plant for more than 10 years prior to being transferred to the pilot-scale column. The anthracite media had been in operation for only 8 months prior to sample collection. Backwashing with unchlorinated filtrate was performed weekly during the study period. Three sets of duplicate GAC samples and a single anthracite sample (n = 7) were collected between October and November of 2016. Details are summarized in Fig. 1, Table 1, and Table S1.

2.1.2. Drinking water treatment plant 2 (DWTP2)

The second study site (DWTP2) was a full-scale drinking water treatment plant with parallel filters containing 183 cm of GAC and 20 cm of sand. These filters were fed with surface water that had been chloraminated to inhibit quagga mussel growth at the intake and then treated with ozone (O_3/DOC = 0.8), ferric chloride coagulation, flocculation, and breakpoint chlorination. The filter influent contained a free chlorine residual of approximately 1.8 mg/L (as Cl_2), although this residual was quenched within the first 50 cm of the GAC bed. The free chlorine was intended to inhibit biological activity in the parallel anthracite filters at this facility (not sampled as part of this study). Samples were collected in November of 2016 from both filters approximately every 15 cm of depth before backwashing (n = 8 from filter 1 and n = 12 from filter 2) and from one of the filters immediately after backwashing (n = 10 from filter 1). Backwashing with chlorinated filtrate was performed weekly during the study period; again, the chlorine was quenched after passing through the sand and bottom layer of the GAC bed. Collectively, these data allow for an assessment of the potential impacts of chlorination, media depth, and backwashing on microbial community structure. Details are summarized in Fig. 1, Table 1, and Table S1.

2.1.3. Reuse pilot 1 (RP1)

The third study site (RP1) was a pilot-scale ozone-biofiltration system containing parallel BAC and anthracite filters and was located on-site at a full-scale wastewater treatment plant. The filters were fed with treated municipal wastewater following full-scale primary clarification, activated sludge treatment (solids retention time of ~7 days, full nitrification, partial denitrification, biological phosphorus removal), secondary clarification, and dual media filtration (anthracite/sand). The tertiary treated wastewater was then ozonated (O_3/DOC = 0.8) and pumped to the three pilot-scale, 15-cm-diameter biofiltration columns (Fig. S1; Module F300, Intuitech, Inc., Salt Lake City, UT). Two columns were packed to a

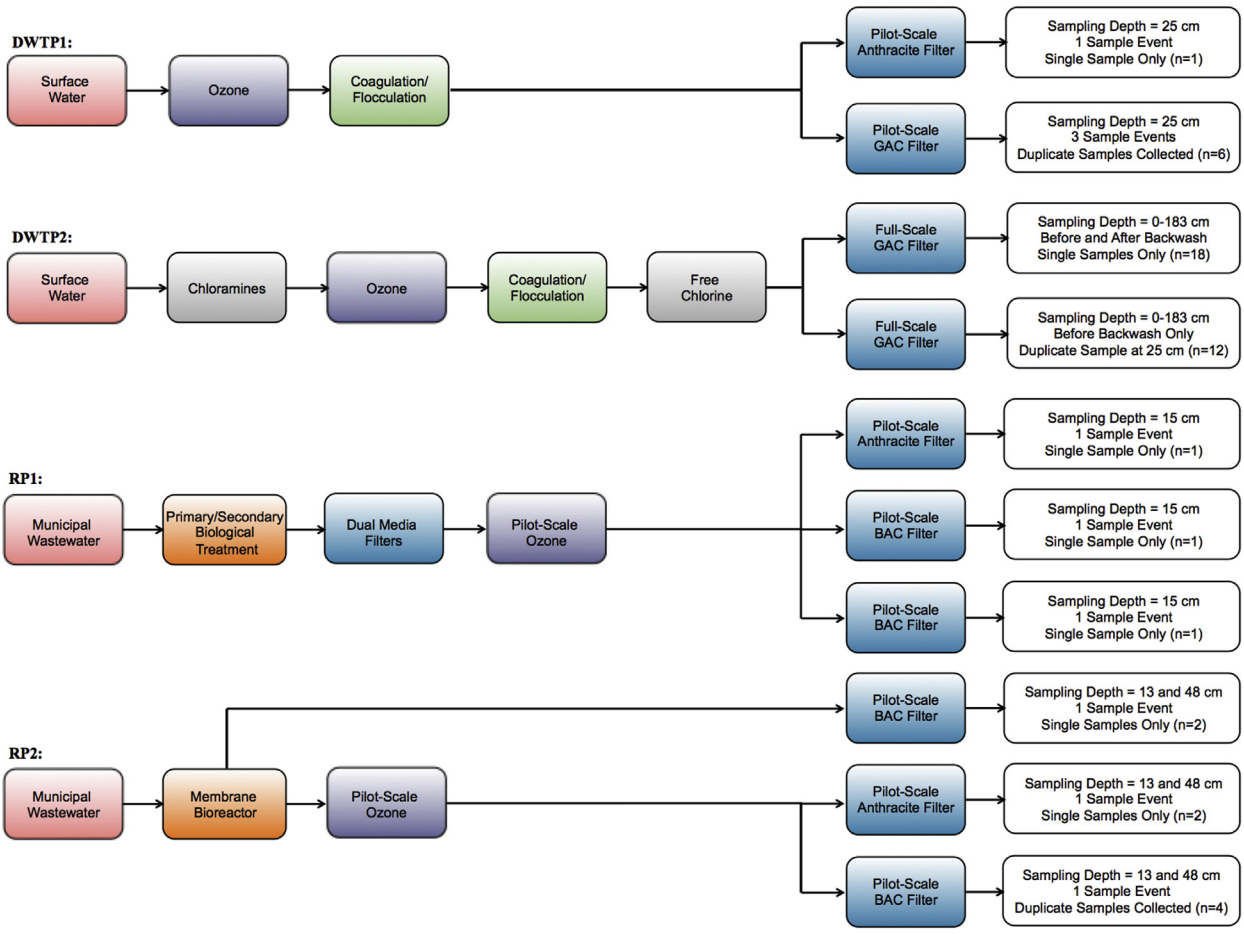

Fig. 1. Schematics and sample breakdown for the treatment trains at the four study sites (DWTP1, DWTP2, RP1, and RP2).

depth of 122 cm with either anthracite or BAC atop 30 cm of sand (EBCT = 10 min). The third column was packed to a depth of 274 cm with BAC atop 30 cm of sand (EBCT = 20 min). The BAC (Norit 820, Cabot Corporation, Alpharetta, GA) had been in operation at the F. Wayne Hill Water Resources Center in Gwinnett County, GA, for over 10 years prior to this study, and exhaustion of the carbon was assumed based on limited DOC removal even when coupled with pre-ozonation (Table 1). Backwashing was performed weekly during the study period. Single samples were collected in October of 2016 from each filter at a depth of 15 cm (n = 3). Details are summarized in Fig. 1, Table 1, and Text S1.

2.1.4. Reuse pilot 2 (RP2)

The fourth study site (RP2) consisted of a pilot-scale ozone-biofiltration system located on-site at a full-scale water reclamation facility. The system was fed with filtrate from a membrane bioreactor (MBR; nominal membrane pore size of 0.04 μm) with a solids retention time of 8–10 days, full nitrification, and partial denitrification. Following ozonation (O_3/DOC = 0.8), the water was pumped into parallel biofiltration columns with diameters of 2.54 cm and bed depths of approximately 76 cm. The columns contained either BAC (Norit 820, Cabot Corporation, Alpharetta, GA) from the F. Wayne Hill Water Resources Center (Gwinnett County, GA; same as RP1) or anthracite provided by the San Jose Creek Water Reclamation Facility (Los Angeles, CA). A separate BAC column was fed with non-ozonated MBR filtrate as a control to evaluate bulk organic removal and microbial community structure in the absence of pre-ozonation. Monthly backwashes with unchlorinated MBR filtrate were sufficient to control head loss accumulation. Samples were collected in July of 2016 from two different depths (13 cm and 48 cm from the surface) in the MBR-ozone-BAC (duplicate), MBR-ozone-anthracite, and MBR-BAC columns (n = 8). Details are summarized in Fig. 1, Table 1, and Text S2.

2.2. Analytical methods

2.2.1. Water quality

Dissolved organic carbon (DOC) was measured as non-purgeable organic carbon according to Standard Method 5310B using a Shimadzu TOC-V_{csn} (Kyoto, Japan). DOC samples were collected in 40-mL amber vials with Teflon-lined lids, filtered with 0.7-μm glass fiber filters (GF/F, Whatman, Pittsburgh, PA), acidified with 2 N hydrochloric acid to reduce the pH to less than 2, and analyzed in duplicate or triplicate.

Organic matter characterization was accomplished with UV (Standard Method 5910B) and fluorescence spectroscopy after sample filtration with 0.7-μm glass fiber filters (GF/F, Whatman, Pittsburgh, PA). Absorbance and fluorescence spectra were generated using an Aqualog spectrofluorometer (Horiba, Edison, NJ) with automated corrections for inner filter effect and Rayleigh masking. Fluorescence data were standardized to the Raman peak area, which was based on an excitation wavelength of 350 nm and emission wavelengths from 380 nm to 410 nm in deionized water. Excitation-emission matrices (EEMs) were then generated using MATLAB (MathWorks, Natick, MA) (Gerrity et al., 2012), and total and regional integrated fluorescence intensities were calculated

Table 1
Descriptions of study sites and average operational conditions (corresponding metadata included in Tables S1 and S2).

Metric	DWTP1	DWTP2	RP1	RP2
No. of Samples	7 samples from two pilot-scale filters	30 samples from two full-scale filters	3 samples from three pilot-scale filters	8 samples from three pilot-scale filters
Water Source and Pretreatment	Surface Water: Ozone, Coagulation, Flocculation	Surface Water: Chloramines, Ozone, Coagulation, Flocculation, Free Chlorine	Wastewater: Activated Sludge, Clarifier, Dual Media Filter, Ozone	Wastewater: MBR, Ozone
Media Type (Age)	GAC (10 + years) and sand; Anthracite (8 months) and sand	GAC (10 + years) and sand	BAC (10 + years); Anthracite (2 years)	BAC (10 + years); Anthracite (4 months)
Acclimation Time Prior to Sampling	8 months	10 + years	4 months	4 months
Filter Depth	(1) 122 cm GAC+30 cm sand (2) 122 cm anthracite+30 cm sand	(1) 183 cm GAC+20 cm sand (2) 183 cm GAC+20 cm sand	(1) 122 cm of anthracite (2) 122 cm of BAC (3) 274 cm of BAC (all: 30 cm sand base)	(1) 76 cm of anthracite (2) 76 cm of BAC (cont.) (3) 76 cm of BAC
Sample Depth from Surface	25 cm	60-183 cm (Filter 1 before BW) 0-183 cm (Filter 1 after BW) 0-183 cm (Filter 2 before BW)	15 cm	High: 13 cm Low: 48 cm
Chlorinated Filtration	No	Free chlorine = 1.8 mg/L Cl_2 (quenched in both filters)	No	No
Chlorinated Backwash	No	Yes	No	No
Backwash Frequency	Weekly	Weekly	Weekly	Monthly
Empty Bed Contact Time	10 min	10-20 min	10 min (152 cm bed) 20 min (304 cm bed)	20 min
O_3/DOC	0.8	0.8	0.8	0 (cont.) 0.8 (ozonated)
Influent DOC (Removal %)	2.4 mg/L (4–8%)	2.4 mg/L (4–8%)	4.8 mg/L (15–18%)	7.8 mg/L (8–20%)
Influent DO	17 mg/L	N/A	30 mg/L	4 mg/L (cont.) 20 mg/L (ozonated)
Influent TIN	0.5 mg-N/L	0.5 mg-N/L	11 mg-N/L	7.6 mg-N/L
Influent PO_4^{3-}	<50 μg/L	<50 μg/L	<50 μg/L	8.7 mg/L

according to Chen et al. (2003). Additional details related to fluorescence analysis and interpretation are provided in Text S3.

Nutrients were also quantified (without laboratory filtration) due to their potential impacts on microbial community structure and function (Li et al., 2010). Ammonia was analyzed with Hach Method 10023 (salicylate method; 0.02–2.5 mg-N/L), nitrite was analyzed with Hach Method 8507 (diazotization method; 0.002–0.3 mg-N/L), nitrate was analyzed with Hach Method 8039 (cadmium reduction method; 0.3–30 mg-N/L), and phosphate was analyzed with Hach Method 8048 (ascorbic acid method; 0.02–2.5 mg/L as PO_4^{-3}). Ammonia, nitrite, and phosphate were measured using a DR900 multiparameter handheld colorimeter (Hach, Loveland, CO), and nitrate was measured using a DR5000 spectrophotometer (Hach, Loveland, CO).

2.2.2. Microbial community characterization

At DWTP1, RP1, and RP2, filter media was extracted from the pilot filters through dedicated sample ports using autoclaved spatulas. At DWTP2, filter media was collected from the full-scale filters using a wheat thief filter coring device (Seedburo Equipment Co., Des Plaines, IL; Fig. S1). For DWTP1, DWTP2, and RP1, media samples were shipped to RTLGenomics (Lubbock, TX) within 24 h of collection. At RTLGenomics, DNA was extracted and purified according to manufacturer protocols using the PowerMag Soil DNA Isolation Kit optimized for the KingFisher platform (MoBio Laboratories, Inc., Carlsbad, CA). The DNA extracts were amplified using degenerate primers targeting the V4-5 region of the 16S rRNA gene (515F: 5′-GTGYCAGCMGCCGCGGTA-3′ and 926R: 5′–CCGYCAATTYMTTTRAGTTT-3′); these primers also target a majority of Archaea (Text S4). For RP2, the DNA was extracted from the filter media within 24 h according to manufacturer protocols using the PowerBiofilm DNA Isolation Kit (MoBio Laboratories, Inc., Carlsbad, CA). The extracted DNA was frozen and shipped to RTLGenomics, where the samples were amplified using degenerate primers targeting the V1-2 region of the 16S rRNA gene (28F: 5′-GAGTTTGATCNTGGCTCAG-3′ and 388R: 5′-TGCTGCCTCCCGTAGGAGT-3′); no Archaea are covered by these primers (Text S4). For both datasets, paired-end sequences were generated at RTLGenomics with a MiSeq sequencer (Illumina, San Diego, CA) using 2 × 300 bp sequencing chemistry. An 8-bp barcode was appended to each set of sequences for identification.

RTLGenomics merged the forward and reverse reads using the paired-end read merger (PEAR) (Zhang et al., 2013) and also performed denoising and chimera checks (Edgar et al., 2011) prior to generating final mapping, multiplexed sequence, and quality files. For DWTP1/DWTP2/RP1, the number of sequences per sample ranged from 8,117 to 32,226, and for RP2, the number of sequences per sample ranged from 32,681 to 143,900. For DWTP1/DWTP2/RP1, the number of bases per sequence ranged from 239 to 449 (average of 374), and for RP2, the number of bases per sequence ranged from 265 to 413 (average of 289). Demultiplexing, quality score filtering, and operational taxonomic unit (OTU) assignment (97% similarity) were performed with Quantitative Insights into Microbial Ecology (QIIME 1) (v. 1.9.1; Caporaso et al., 2010), while downstream processing of raw data, including statistical analyses, visualization, and taxonomic assignments, was performed with QIIME 2 (v. 2017.6; Caporaso, 2017). Data processing included rarefaction at a sampling depth of 8,117 sequences for DWTP1/DWTP2/RP1 and 32,681 sequences for RP2 followed by the computation of alpha and beta diversity metrics. Assignment of taxonomy was accomplished with a naïve Bayesian classifier trained on the 97% majority SILVA (release 128) database (Quast et al., 2013). Changes in differential abundance were evaluated using Analysis of Composition of Microbiomes (ANCOM) (Mandal et al., 2015).

Additional details related to DNA extraction, primer coverage, and the data analysis pipeline are summarized in Text S4. Merged paired reads, provided by RTLGenomics, are available from the European Nucleotide Archive under Study Accession Number

PRJEB22574.

3. Results and discussion

3.1. General water quality

The general water qualities of the various feed waters are summarized in Table 1. The filters at DWTP1 and DWTP2 received relatively high quality surface water with low nutrient and bulk organic matter concentrations [total inorganic nitrogen (TIN) ≈ 0.5 mg-N/L, orthophosphate < 50 μg/L, and DOC ≈ 2.4 mg/L]. Pre-ozonation with an O_3/DOC ratio of 0.8 was expected to convert some of the recalcitrant natural organic matter into biodegradable dissolved organic carbon (BDOC; Ratpukdi et al., 2010), thereby providing a carbon source/electron donor for the microbial community. The two wastewater matrices (RP1 and RP2) contained higher concentrations of bulk organic matter (DOC ≈ 4.8–7.8 mg/L) and nitrogen (TIN ≈ 8-11 mg-N/L), but the orthophosphate concentration ranged from <50 μg/L for RP1 (due to chemical and biological phosphorus removal) to 8.7 mg/L for RP2. Despite the higher DOC concentrations in the two wastewaters, the bulk organic matter was expected to be biologically recalcitrant due to upstream biological treatment. Again, ozonation with an O_3/DOC ratio of 0.8 likely converted the recalcitrant bulk organic matter into more bioavailable fractions (Ratpukdi et al., 2010), except for the RP2 'control' BAC column receiving non-ozonated MBR filtrate.

Representative EEMs for drinking water (DWTP2) and wastewater (RP2) matrices are shown in Fig. 2. The difference in fluorescence intensity for the raw surface water versus the MBR filtrate is representative of the greater quantity and complexity of the bulk organic matter present in the wastewater matrix. The reductions in total fluorescence intensity after ozonation (75% and 88%, respectively; Table S3) represent the bulk organic matter transformation achieved via ozone and •OH radical oxidation.

In contrast with the reduction in fluorescence intensity achieved by ozonation, there was an increase in fluorescence intensity observed in both systems after biofiltration (i.e., in the GAC/BAC effluents; Table S3), presumably due to the release of extracellular polymeric substances (EPS) by the microbial community. The increases were particularly notable for region I (+108% and +174%, respectively; Table S3), but there were also prominent increases in peak fluorescence for both systems at excitation/emission wavelengths of 295/410 nm (Fig. 2). In contrast, the total fluorescence in the 'control' BAC effluent with no pre-ozonation exhibited a 17% decrease relative to the MBR filtrate (data not shown).

The synergistic combination of ozone and biofiltration is effective for achieving net removal of bulk organic matter (Table 1; Arnold et al., 2018). Moreover, it may be possible to maximize total organic carbon (TOC) removal by identifying critical EPS-producers (Subramanian et al., 2010) and minimizing their abundance via operational modifications. This is also important because EPS has been identified as an important source of disinfection byproduct (DBP) precursors (Liu et al., 2017). Potential improvements in biofiltration performance and effluent water quality justify the use of advanced molecular methods (e.g., 16S rRNA gene sequencing) to highlight relationships between design/operational criteria and microbial community structure. The following sections attempt to identify some of these relationships.

3.2. Alpha (Intra-sample) diversity metrics

3.2.1. DWTP1, DWTP2, and RP1

A summary of alpha diversity metrics for DWTP1, DWTP2, and RP1 is shown in Table S5. The Chao1 metric—a statistical estimate of total OTU richness—was always consistent with observed OTU richness, which suggests that adequate sequencing depth was achieved for all samples. All samples also exhibited high alpha

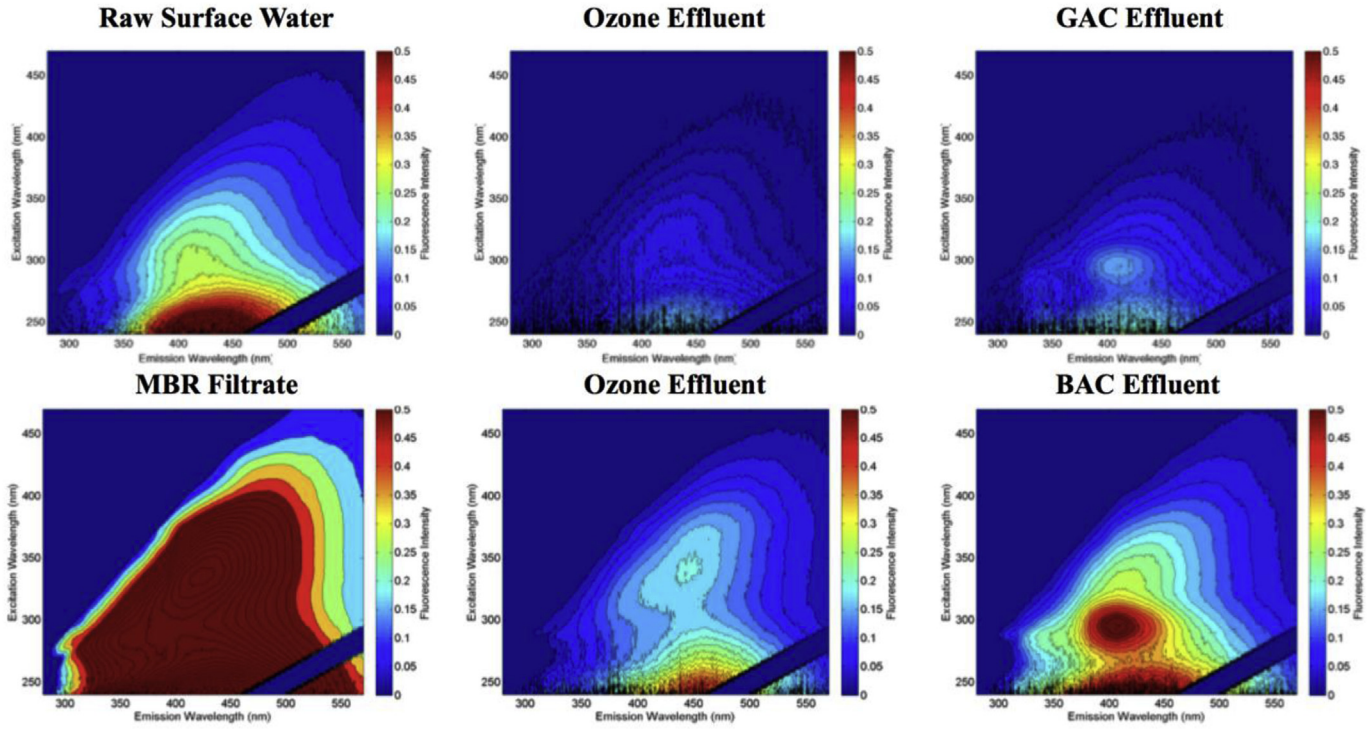

Fig. 2. Excitation emission matrices (EEMs) characterizing the dissolved organic matter at various stages of treatment in (top) DWTP2 and (bottom) RP2. Additional information (e.g., total and regional fluorescence intensities) is included in Text S3.

diversity based on the Shannon and Simpson indices. The Shannon index simultaneously accounts for OTU richness and evenness, while the Simpson index is less sensitive to richness and gives the probability that any two randomly selected individuals will belong to different OTUs (Hill, 1973). The Shannon indices were generally consistent with soil microbial communities in the literature (i.e., ≈4.5; Hill et al., 2003), but notable exceptions included the GAC (considerably higher at 5.8) and anthracite (considerably lower at 3.9) filters at DWTP1. This was due to the corresponding differences in OTU richness for these two groups relative to the overall dataset. Besides the difference in media type, the only difference between the GAC and anthracite at DWTP1 was that the GAC had been in use for 10 + years prior to being transferred to the pilot, while the anthracite had only been in use for 8 months. The GAC filters at DWTP2 generally had lower alpha diversity compared to the GAC at DWTP1, thereby suggesting that alpha diversity may be facility-specific. High alpha diversity (Shannon index > 6.0 and Simpson index > 0.96) was observed for one of the BAC filters and the anthracite filter at RP1, but it is unclear why the second BAC filter did not have similarly high alpha diversity (Shannon index = 4.6 and Simpson index = 0.83).

Results of Kruskal-Wallis (or two-sample *t*-test) alpha diversity comparisons (richness, evenness, Shannon index, and Faith's phylogenetic diversity) are summarized in Table S6. Faith's phylogenetic diversity (PD) provides an indication of the total branch length of a sample's corresponding phylogenetic tree. Media type, mode (filter vs. backwash), and depth had no significant impacts on alpha diversity. However, significant differences ($p < 0.05$) were observed when controlling only for facility or water type (wastewater vs. drinking water). All alpha diversity metrics were significantly higher for DWTP1 in comparison with DWTP2, while DWTP1 and RP1 only differed for OTU richness and Faith's PD (RP1 was higher in both instances).

3.2.2. RP2

Summaries of the aforementioned alpha diversity metrics for RP2 are shown in Tables S7 and S8. Similar to RP1, OTU richness for the RP2 samples was considerably higher than the drinking water facilities in the first dataset. However, the Shannon and Simpson indices for RP2 were generally lower than those of RP1, thereby suggesting community dominance by fewer types of bacteria. The Kruskal-Wallis (or *t*-test) results indicated that ozonation led to significantly reduced OTU richness ($p = 0.05$) and alpha diversity based on Faith's PD ($p = 0.05$) but not for evenness ($p = 0.50$) or Shannon index ($p = 0.18$). Media type had no significant impacts on alpha diversity in RP2, but increasing depth led to significant increases in evenness ($p = 0.04$). These results indicate that there may be a slight positive correlation between operational stress, specifically a reduction in BDOC due to lack of pre-ozonation or increased retention time, and alpha diversity in wastewater filters, which is consistent with Li et al. (2012).

3.3. Beta (Inter-sample) diversity metrics

3.3.1. DWTP1, DWTP2, and RP1

Abundance-unweighted UniFrac distances and abundance-weighted Bray Curtis dissimilarities were used to compare beta diversity for DWTP1, DWTP2, and RP1 (Fig. 3). In these plots, the relative positioning of each data point (i.e., sample) provides an indication of the similarity of its microbial community to that of other samples in the dataset. The corresponding permutational analysis of variance (PERMANOVA) statistics are summarized in Table S9.

When focusing only on phylogeny (i.e., unweighted UniFrac), all of the samples clustered tightly by facility, with no clear visual impacts from backwashing or depth. There were clear differences between DWTP1 and DWTP2, thereby indicating that factors other than water type (i.e., wastewater vs. drinking water) had a significant impact on microbial community structure. There was a slight impact due to media type at DWTP1, with anthracite as the visually apparent outlier (Fig. 3), but not at RP1.

When focusing only on abundance (i.e., Bray Curtis), the samples from DWTP1 were relatively similar, but with anthracite still appearing as an outlier. However, there was considerable separation in the DWTP2 samples. The differences did not appear to be related to backwashing, which suggested that depth was potentially impacting microbial community structure. To further evaluate this issue, the unweighted UniFrac and weighted Bray Curtis analyses were repeated as a function of depth (Fig. 4). Both analyses showed that there were slight, albeit insignificant, differences in microbial community structure at greater depths in the GAC filters at DWTP 2 ($p \approx 0.10$ for all pairwise PERMANOVAs for the reference depth of 183 cm). A similar visual trend was apparent in the Bray Curtis data near the surface of the GAC. This may have been related to the effects of free chlorine penetration (during filtration and backwashing) prior to complete quenching.

Finally, the three samples from RP1 were tightly clustered for the UniFrac and Bray Curtis analyses (Figs. 3 and 4), thereby indicating minimal differences in beta diversity (if any) resulting from varying media type at RP1.

3.3.2. RP2

Abundance-unweighted UniFrac distances and abundance-weighted Bray Curtis dissimilarities were also used to evaluate beta diversity for RP2 (Fig. 3), and the corresponding PERMANOVA results are summarized in Table S9. Potential differences due to operational conditions were more visually apparent for RP2 because the samples were not impacted by the potentially confounding effects of water type or facility. Despite one outlier (duplicate for ozone-BAC-low/deep), the UniFrac and Bray Curtis beta diversity metrics indicated that neither depth ($p = 0.74$ and $p = 0.53$, respectively) nor pre-ozonation ($p = 0.11$ and $p = 0.20$, respectively) had a significant impact on beta diversity in RP2. Depth may not have been a significant factor for beta diversity at RP2 because of the lack of disinfectant residual and the greater nutrient and BDOC loading in the feedwater, at least in comparison with DWTP2 (the only other facility sampled at multiple depths). Similar to DWTP1, media type ($p = 0.04$ for UniFrac and $p = 0.03$ for Bray Curtis) did have a significant impact on beta diversity, which is interesting because BAC often achieves greater TOC removal than anthracite despite similar biomass density (Arnold et al., 2018).

3.4. Overview of abundant taxa at the phylum level

The preceding sections described differences in alpha and beta diversity as a function of various water quality and operational variables. The following sections describe the taxonomic differences contributing to those statistical observations. Full OTU tables are also provided as SI files.

3.4.1. DWTP1, DWTP2, and RP1

Relative abundance at the phylum level for the samples collected from DWTP1/DWTP2/RP1 is summarized in Fig. 5. The phylum Proteobacteria, which consists of a wide variety of pathogenic and non-pathogenic bacteria, was the most abundant phylum, comprising more than 65% of the microbial community in every sample except those collected from RP1. The samples from DWTP1, DWTP2, and RP1 exhibited considerable variability with respect to the remaining phyla. The anthracite filter at DWTP1 was composed of >90% Proteobacteria but also contained a greater

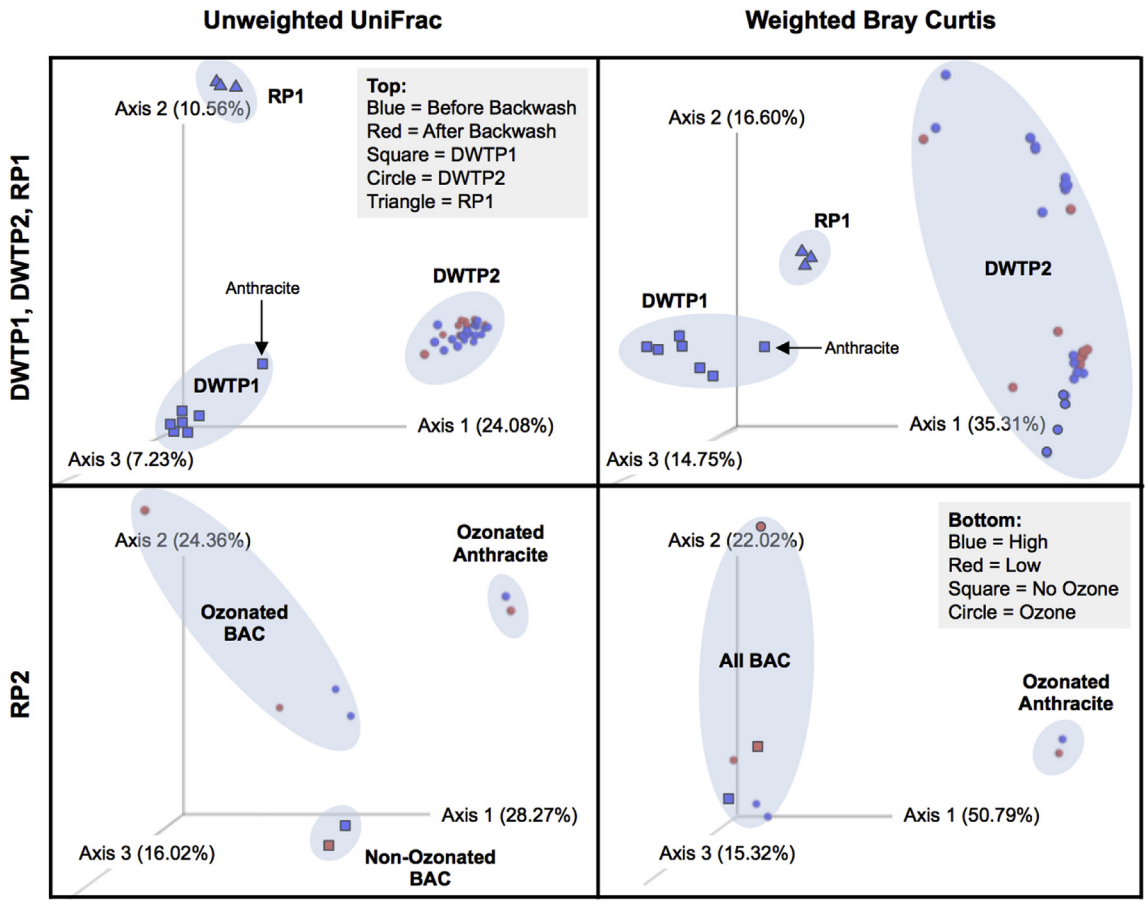

Fig. 3. Principal coordinate analyses (PCoAs) for (top) DWTP1/DWTP2/RP1 and (bottom) RP2. The left side of the figure represents the abundance-unweighted UniFrac distances between datasets, and the right side of the figure represents the abundance-weighted Bray Curtis distances between datasets. The percentages along the axes represent the percent variability explained by the ordination.

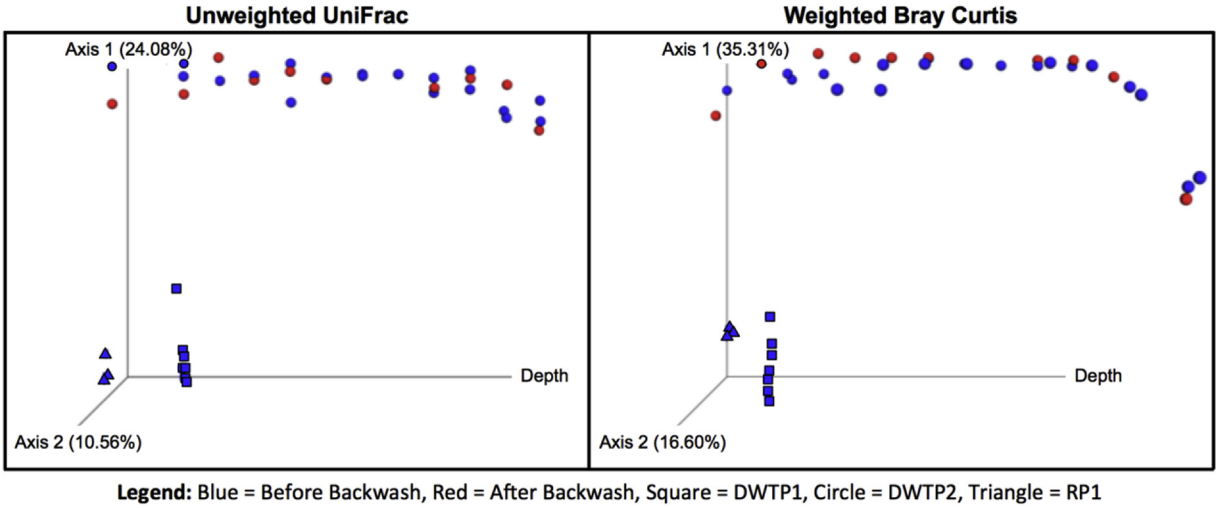

Fig. 4. Principal coordinate analyses (PCoAs) for all samples from DWTP1, DWTP2, and RP1 as a function of depth. All samples from DWTP1 and RP1 were collected from a depth of 15 cm or 25 cm, and samples from DWTP2 were collected from depths ranging from 0 cm to 183 cm (before and after backwash). The left side of the figure represents the abundance-unweighted UniFrac distances between datasets, and the right side of the figure represents the abundance-weighted Bray Curtis distances between datasets. The percentages along axes 1 and 2 represent the percent variabilities explained by the ordination, and the third axis represents depth within the filter column.

relative abundance of Cyanobacteria (3.11%) compared to the replicate samples from the parallel GAC filter (0.65 ± 0.21%). The GAC filter contained only 75% Proteobacteria but contained relatively large fractions of Bacteroidetes (5.31 ± 1.08%), Acidobacteria (9.15 ± 3.72%), Planctomycetes (5.35 ± 1.42%), and Nitrospirae (3.14 ± 1.03%); the differential abundance of Acidobacteria in

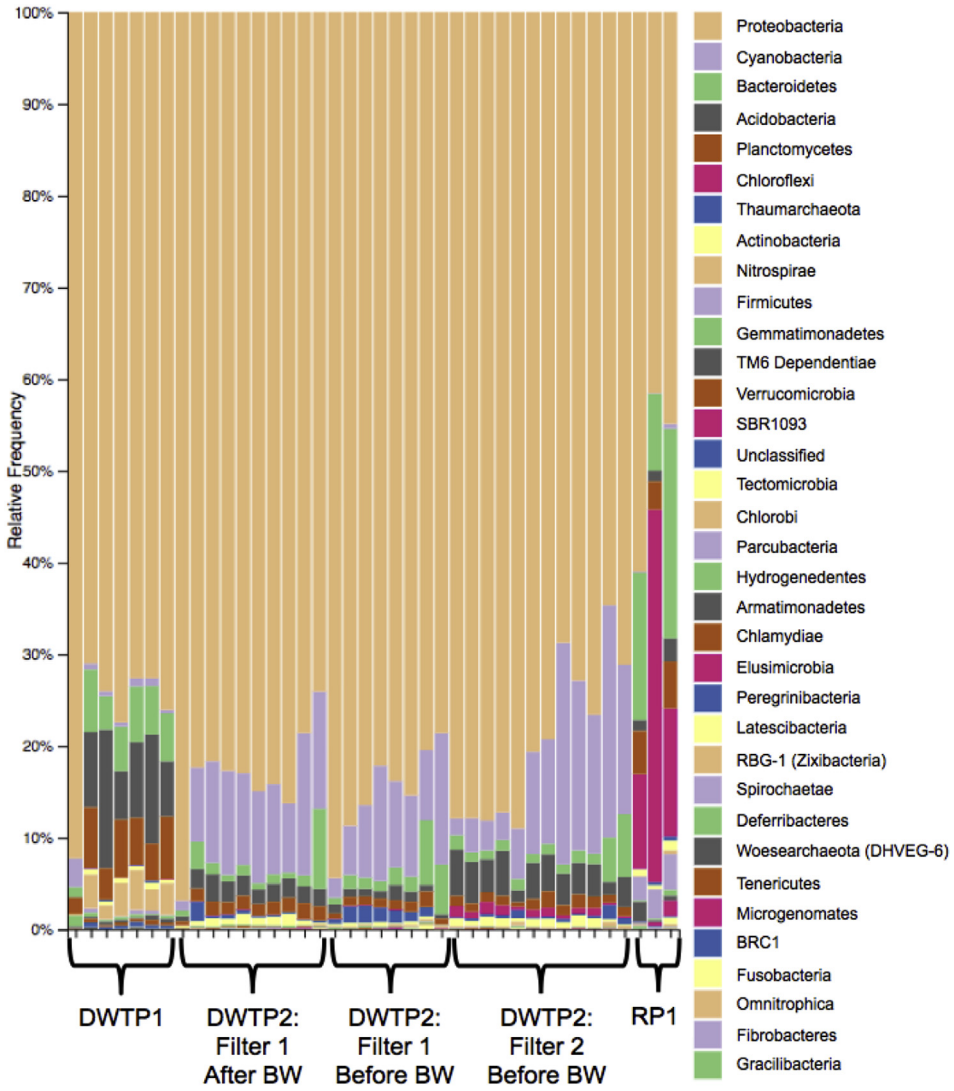

Fig. 5. Taxa bar plot at the phylum level for DWTP1, DWTP2, and RP1. Phyla are listed in descending order of relative abundance for the overall dataset. The bars for DWTP2 are listed in order of depth (i.e., shallow to deep). The first bars for DWTP1 and RP1 represent anthracite filters, and all others represent GAC or BAC filters for the drinking water and wastewater facilities, respectively. BW = backwash.

GAC samples was also confirmed by ANCOM. Bacteroidetes and Acidobacteria are commonly observed in soil ecosystems, but their ecological roles are still unclear (Eichorst et al., 2007), in part because of difficulties in culturing these bacteria (Kielak et al., 2016). Planctomycetes are known to contain complex intracellular compartments—analogous to eukaryotic organelles—including the anammoxosome responsible for nitrification (Fuerst and Sagulenko, 2011). Finally, the Nitrospirae are known nitrite oxidizers (Lucker et al., 2010).

Consistent with the GAC at DWTP1, DWTP2 was dominated by Proteobacteria and exhibited a high relative abundance of Acidobacteria, both of which are common to soil environments. As confirmed by ANCOM, Cyanobacteria were also highly abundant, particularly at greater depths. The Cyanobacteria were primarily from the class Melainabacteria, which are non-photosynthetic, anaerobic, nitrogen fixers (Di Rienzi et al., 2013). Importantly, they also differ from the Cyanobacteria responsible for cyanotoxin production (Blaha et al., 2009). Melainabacteria are known to occur in the human gut, where they have been linked to fermentation and vitamin synthesis (Soo et al., 2014), but their role in drinking water filters is unclear. The occurrence of Cyanobacteria in some of the drinking water filters may have been related to low nitrogen levels, thereby promoting nitrogen fixation, or potentially higher ambient levels of Cyanobacteria in the source water, thereby allowing for filter colonization.

Filter 1 at DWTP2 contained a noticeable amount of Thaumarchaeota prior to backwashing but not after backwashing (Fig. 5). Thaumarchaeota were also present in Filter 2, although their relative abundance was visually attenuated in Fig. 5 due to the greater prevalence of Acidobacteria. Thaumarchaeota are Archaea known to thrive in low-ammonia environments (Pester et al., 2011); no ammonia was expected at DWTP2 due to breakpoint chlorination being performed prior to filtration. On the other hand, the phylum Planctomycetes exhibited a slightly higher relative abundance following filter backwashing, which is consistent with Kasuga et al. (2007). Interestingly, ANCOM identified the phylum Chlamydiae as being differentially abundant immediately following a filter backwash, although these bacteria were not particularly abundant overall. Certain bacterial species from the phylum Chlamydiae (*Neochlamydia hartmannellae*) are known endosymbionts

of free-living amoebae (e.g., *Acanthamoeba* and *Hartmannella*) (Horn et al., 2000). Therefore, amoebae present in the filters may harbor these bacteria and prevent them from being eliminated during backwashing.

In contrast with the drinking water filters, Proteobacteria only comprised 40–45% and 60% of the microbial communities in the BAC and anthracite filters, respectively, at RP1. Some Proteobacteria appear to exhibit a competitive advantage in systems with low DOC concentrations (Eiler et al., 2003), which might explain their greater relative abundance in drinking water versus wastewater filters. The wastewater filters were instead characterized by high relative abundance of Firmicutes and Chloroflexi according to ANCOM and also Bacteroidetes and Planctomycetes. Firmicutes and Bacteroidetes are considered "core microbiota" of the human gut (Caporaso et al., 2011), and Planctomycetes (Fuerst and Sagulenko, 2011) and Chloroflexi (Bjornsson et al., 2002) have been linked to biological nutrient removal systems. Recall that RP1 is fed with full-scale secondary wastewater effluent from an activated sludge system targeting full nitrification, partial denitrification, and biological phosphorus removal.

3.4.2. RP2

The experimental setup at RP2 allowed for a more targeted evaluation of microbial community structure in wastewater systems because it directly compared the effects of pre-ozonation, media type, and media depth at a single wastewater facility. A taxa bar plot at the phylum level is provided in Fig. 6. Similar to DWTP1 and DWTP2, but interestingly in slight contrast with RP1, Proteobacteria comprised an overwhelming majority of the microbial community in RP2. In fact, Proteobacteria comprised as much as 95% of the microbial community near the surface of the ozonated BAC column. A potential explanation for the difference in relative abundance of Proteobacteria between RP1 and RP2 is discussed later in the context of genus-level characterization. Also in contrast with RP1, the filters at RP2 were characterized by low relative abundance of Firmicutes and high relative abundance of Actinobacteria. Similar to RP1, all of the filters at RP2 were abundant in Chloroflexi and to a lesser degree Bacteroidetes. Bacteroidetes have been linked to degradation of high molecular weight organic compounds (Thomas et al., 2011), which are expected to be abundant in wastewater. This might portend a greater relative prevalence in the absence of pre-ozonation (i.e., the control BAC column), but this was not observed at RP2 (Fig. 6). Instead, Bacteroidetes exhibited the greatest relative prevalence in the ozone-anthracite system. Alternatively, Bacteroidetes may be more prevalent in wastewater filters simply because of their role in the human digestive system.

With respect to differential abundance between RP2 samples, there were three notable observations: (1) ANCOM identified Phylum SBR1093 as having high relative abundance in BAC, (2) Bacteroidetes exhibited high relative abundance in anthracite, and (3) Nitrospirae were differentially abundant in the 'control' BAC filter receiving non-ozonated MBR filtrate. Again, these bacteria are described as nitrite-oxidizing bacteria (Lucker et al., 2010) and are found in a variety of natural and engineered environments (Daims et al., 2015). The nitrite concentration in the MBR filtrate was 0.2 ± 0.1 mg-N/L, but it was an order of magnitude lower (0.02 ± 0.03 mg-N/L) in the ozonated MBR filtrate, presumably because nitrite is known to react rapidly with ozone (Lee et al., 2013). Therefore, the higher nitrite concentration in the MBR filtrate feeding the 'control' filters may explain the higher relative prevalence of Nitrospirae.

3.5. Overview of abundant taxa at the genus level

The most abundant OTUs present in eight representative samples from DWTP1/DWTP2/RP1 are summarized in Table 2, and the 20 OTUs that were present in all 40 samples from that dataset are summarized in Table 3. Similar to the "core microbiota" of the human gut (Caporaso et al., 2011), Table 3 highlights the core microbiota of the drinking water and wastewater filters in the current study, although some of the relative abundances still differ considerably between samples. Some of these taxa, such as *Hyphomicrobium*, Planctomycetales (order), and Burkholderiales (order), have also been identified as abundant taxa in other biofiltration studies (Li et al., 2017). Finally, the most abundant OTUs for RP2 are summarized in Table 4. The potential significance of many of these bacteria was summarized previously in the discussion of abundant phyla so the following sections focus only on several genera of interest.

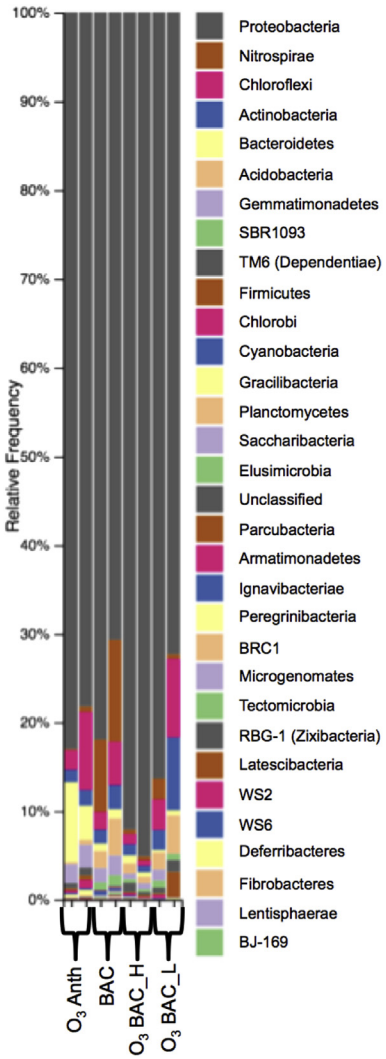

Fig. 6. Taxa bar plot at the phylum level for RP2. Phyla are listed in descending order of relative abundance for the overall dataset. The first bars for the O_3-anthracite and BAC (no preozonation) pairs represent samples collected high in the column (i.e., shallow). The O_3-BAC samples were collected in duplicate for the high (H; shallow) and low (L; deep) sample ports.

3.5.1. Genera Neochlamydia and Legionella in DWTP2

The phylum Chlamydiae was previously identified as being differentially abundant following backwashing at DWTP2. This differential abundance was subsequently linked to a genus-level OTU classified as *Neochlamydia*, which is an endosymbiont linked

Table 2
Most abundant OTUs in representative samples from DWTP1, DWTP2, and RP1, all of which employed ozonation. Collectively, these OTUs represent the top 10 in each sample. "BW" indicates samples collected immediately following a backwash cycle, and "high" and "low" designate depths less than 30 cm and greater than 150 cm, respectively. Asterisks indicate that taxonomic rank refers to order instead of genus (due to incomplete classification).

Phylum	Genus	DWTP1 GAC High	DWTP1 Anth. High	DWTP2 GAC High	DWTP2 GAC Low	DWTP2 GAC_BW High	DWTP2 GAC_BW Low	RP1 BAC High	RP1 Anth. High
Proteobacteria	Methylophilales*	19.02%	10.53%	0.00%	0.00%	0.00%	0.00%	0.00%	0.00%
Proteobacteria	Burkholderiales*	13.77%	41.47%	51.48%	26.19%	7.34%	4.67%	2.04%	3.27%
Proteobacteria	*Hyphomicrobium*	4.27%	1.20%	3.00%	3.65%	2.70%	3.00%	0.96%	1.09%
Nitrospirae	*Nitrospira*	3.40%	0.11%	0.06%	0.06%	0.01%	0.01%	0.05%	0.04%
Proteobacteria	Rhizobiales*	3.06%	1.70%	0.15%	1.53%	0.90%	1.57%	0.09%	0.30%
Proteobacteria	*Nitrosomonas*	2.72%	2.65%	0.00%	0.00%	0.00%	0.00%	0.00%	0.00%
Proteobacteria	*Reyranella*	2.38%	7.05%	6.50%	6.90%	10.84%	8.57%	4.15%	3.03%
Acidobacteria	Blastocatellales*	2.12%	0.00%	0.05%	0.16%	0.06%	0.19%	0.19%	0.04%
Proteobacteria	TRA3-20*	1.68%	6.25%	2.08%	4.11%	7.16%	4.72%	0.48%	0.96%
Proteobacteria	*Bradyrhizobium*	1.63%	0.73%	1.49%	1.87%	4.52%	7.15%	1.72%	2.94%
Planctomycetes	*Planctomyces*	1.63%	0.02%	0.17%	0.12%	0.11%	0.46%	1.90%	2.91%
Proteobacteria	*Nannocystis*	1.60%	2.15%	0.00%	0.03%	0.00%	0.00%	0.00%	0.00%
Proteobacteria	*Rhodobacter*	1.25%	0.43%	0.20%	2.41%	1.02%	2.59%	0.00%	0.04%
Proteobacteria	Nitrosomonadales*	0.91%	0.03%	4.77%	1.95%	3.85%	2.65%	0.43%	0.66%
Bacteroidetes	*Terrimonas*	0.73%	0.00%	0.00%	0.75%	0.11%	0.24%	5.31%	6.87%
Proteobacteria	Rhodospirillales*	0.64%	0.05%	3.47%	4.42%	13.14%	9.58%	0.60%	0.39%
Proteobacteria	*Variibacter*	0.54%	0.00%	0.83%	1.05%	7.98%	7.28%	0.36%	0.10%
Proteobacteria	Rhodocyclales*	0.47%	1.51%	0.00%	0.00%	0.00%	0.01%	0.42%	0.69%
Cyanobacteria	Obscuribacterales*	0.36%	3.01%	2.10%	7.43%	11.25%	15.46%	0.03%	0.12%
Proteobacteria	Rhizobiales*	0.22%	0.03%	0.04%	0.06%	0.67%	0.66%	1.33%	3.17%
Proteobacteria	*Legionella*	0.19%	0.83%	0.18%	0.81%	2.25%	4.75%	0.08%	0.10%
Bacteroidetes	Flavobacteriales*	0.14%	0.00%	0.11%	4.13%	0.16%	0.28%	0.00%	0.00%
Proteobacteria	*Arenimonas*	0.11%	0.10%	0.00%	0.00%	0.00%	0.00%	4.00%	6.47%
Proteobacteria	*Sphingopyxis*	0.09%	0.02%	0.02%	0.20%	0.04%	0.16%	0.63%	3.58%
Proteobacteria	Rhizobiales*	0.09%	0.00%	0.00%	0.00%	0.00%	0.01%	2.74%	2.04%
Proteobacteria	*Sphingomonas*	0.04%	0.02%	1.30%	4.13%	0.31%	0.51%	0.05%	0.51%
Proteobacteria	Sphingomonadales*	0.01%	3.05%	0.00%	0.00%	0.00%	0.00%	1.31%	3.64%
Chloroflexi	Caldilineales*	0.00%	0.00%	0.00%	0.00%	0.00%	0.00%	40.25%	8.50%
Proteobacteria	*Thermomonas*	0.00%	0.00%	0.00%	0.00%	0.00%	0.00%	1.61%	6.17%
Proteobacteria	*Meganema*	0.00%	0.00%	0.00%	0.00%	0.00%	0.00%	5.33%	0.77%
Proteobacteria	*Sphingorhabdus*	0.00%	0.00%	13.48%	6.44%	7.06%	5.64%	0.00%	0.00%
Other	Other	37%	17%	8.5%	22%	19%	20%	24%	42%

Table 3
Relative abundance of the 20 OTUs that were present in all 40 samples from DWTP1, DWTP2, and RP1. The data represent means ± 1 standard deviation. Asterisks indicate that taxonomic rank refers to order instead of genus (due to incomplete classification).

Phylum	Genus	DWTP1	DWTP2 (F1)	DWTP2 (BW1)	DWTP2 (F2)	RP1
Proteobacteria	Burkholderiales*	17.09 ± 10.82%	30.11 ± 9.50%	8.28 ± 4.97%	11.45 ± 13.38%	2.36 ± 0.80%
Proteobacteria	*Reyranella*	5.20 ± 2.23%	7.34 ± 2.88%	9.12 ± 3.05%	16.07 ± 7.82%	2.49 ± 1.99%
Proteobacteria	TRA3-20*	3.64 ± 1.97%	4.13 ± 1.64%	5.16 ± 1.96%	7.12 ± 2.80%	0.86 ± 0.35%
Proteobacteria	*Hyphomicrobium*	3.31 ± 1.24%	3.36 ± 0.39%	3.16 ± 0.42%	4.33 ± 1.08%	1.23 ± 0.37%
Proteobacteria	*Bradyrhizobium*	1.10 ± 0.39%	1.86 ± 0.59%	7.60 ± 7.20%	5.58 ± 2.67%	2.46 ± 0.65%
Proteobacteria	Rhizobiales*	0.97 ± 0.53%	0.18 ± 0.07%	0.26 ± 0.08%	0.29 ± 0.14%	0.41 ± 0.25%
Cyanobacteria	Obscuribacterales*	0.93 ± 0.94%	8.46 ± 3.85%	9.68 ± 3.77%	11.58 ± 8.35%	0.22 ± 0.25%
Bacteroidetes	Cytophagales*	0.82 ± 0.25%	0.16 ± 0.10%	0.16 ± 0.17%	0.13 ± 0.13%	0.41 ± 0.33%
Proteobacteria	Rhodospirillales*	0.80 ± 0.44%	4.46 ± 1.47%	11.01 ± 5.78%	8.07 ± 3.20%	0.61 ± 0.22%
Proteobacteria	Nitrosomonadales*	0.74 ± 0.38%	3.14 ± 1.30%	3.11 ± 0.98%	0.85 ± 0.26%	0.85 ± 0.54%
Proteobacteria	*Pedomicrobium*	0.56 ± 0.33%	0.06 ± 0.05%	0.14 ± 0.08%	0.18 ± 0.11%	0.68 ± 0.43%
Proteobacteria	*Amphiplicatus*	0.49 ± 0.25%	0.62 ± 0.54%	0.99 ± 1.15%	0.94 ± 0.87%	0.26 ± 0.21%
Planctomycetes	Planctomycetales*	0.45 ± 0.22%	0.27 ± 0.18%	0.67 ± 0.26%	0.44 ± 0.26%	0.58 ± 0.28%
Gemmatimonadetes	Gemmatimonadales*	0.43 ± 0.36%	0.12 ± 0.05%	0.12 ± 0.05%	0.06 ± 0.03%	0.31 ± 0.29%
Acidobacteria	Blastocatellales*	0.40 ± 0.18%	0.25 ± 0.16%	0.33 ± 0.19%	0.22 ± 0.11%	0.52 ± 0.40%
Proteobacteria	*Legionella*	0.32 ± 0.25%	0.53 ± 0.30%	3.01 ± 1.66%	1.31 ± 0.68%	0.06 ± 0.05%
Proteobacteria	TRA3-20*	0.32 ± 0.27%	0.23 ± 0.21%	0.39 ± 0.61%	0.09 ± 0.08%	0.06 ± 0.06%
Proteobacteria	Rickettsiales*	0.31 ± 0.18%	0.21 ± 0.14%	0.13 ± 0.08%	0.09 ± 0.04%	0.15 ± 0.13%
Proteobacteria	Rhizobiales*	0.29 ± 0.28%	0.08 ± 0.04%	0.63 ± 0.37%	0.18 ± 0.11%	1.77 ± 1.24%
Proteobacteria	Rickettsiales*	0.22 ± 0.33%	0.58 ± 0.20%	1.14 ± 0.39%	1.81 ± 0.62%	0.06 ± 0.04%
Other	Other	62%	34%	35%	29%	84%

to free-living *Acanthamoeba* and *Hartmannella* (Horn et al., 2000). Interestingly, as part of a follow-up study, de Vera et al. (2018) observed an unexpected spike in *Acanthamoeba* concentration in the effluent from this same filter. Despite being differentially abundant after backwashing, *Neochlamydia* was still rare (<0.5% abundance) relative to the overall microbial community. On the other hand, *Legionella*—a pathogenic endosymbiont (Khan, 2006) that is critically important to human health—exhibited greater relative abundance after backwashing and also comprised up to 5% of the microbial community in some samples (Table 2). Prior to

Table 4
Most abundant OTUs in all samples from RP2. Collectively, these OTUs represent the top 10 in each sample. Asterisks indicate that taxonomic rank refers to order instead of genus, and "N/A" indicates that classification was limited to the phylum level (both due to incomplete classification).

Phylum	Genus	Control BAC High	Control BAC Low	Ozone BAC High_1	Ozone BAC High_2	Ozone BAC Low_1	Ozone BAC Low_2	Ozone Anth. High	Ozone Anth. Low
Proteobacteria	*Bradyrhizobium*	41.54%	22.43%	58.74%	60.78%	19.28%	40.05%	18.87%	19.55%
Proteobacteria	Rhodospirillales*	8.51%	7.42%	3.62%	5.36%	5.54%	6.30%	0.53%	0.85%
Nitrospirae	*Nitrospira*	8.14%	11.48%	0.49%	0.46%	0.52%	2.26%	0.14%	0.62%
Proteobacteria	Rhodospirillales*	4.40%	3.88%	3.32%	4.19%	19.48%	5.25%	0.31%	0.65%
Proteobacteria	Rhodospirillales*	3.53%	2.58%	3.05%	2.91%	2.35%	4.69%	0.01%	0.04%
Proteobacteria	*Pedomicrobium*	2.41%	3.00%	2.00%	1.34%	1.04%	1.92%	0.75%	1.10%
Proteobacteria	Xanthomonadales*	1.58%	1.59%	1.25%	1.00%	0.52%	1.30%	0.01%	0.02%
Gemmatimonadetes	Gemmatimonadales*	1.52%	1.96%	0.55%	0.56%	0.00%	1.12%	1.18%	1.12%
Proteobacteria	*Hyphomicrobium*	1.29%	0.56%	0.98%	1.03%	0.00%	1.95%	0.69%	1.27%
Proteobacteria	*Variibacter*	1.14%	2.04%	2.55%	2.19%	3.41%	4.52%	0.40%	3.06%
Proteobacteria	Burkholderiales*	1.07%	3.45%	1.95%	2.49%	2.83%	2.42%	20.72%	8.39%
Proteobacteria	TRA3-20*	1.04%	1.22%	1.64%	2.90%	1.67%	3.16%	4.07%	5.37%
Proteobacteria	Nitrosomonadales*	0.61%	2.65%	0.22%	0.89%	0.30%	1.00%	11.32%	7.65%
Proteobacteria	Rhizobiales*	0.59%	0.84%	0.87%	0.59%	0.35%	0.54%	2.10%	2.89%
Proteobacteria	Rhizobiales*	0.55%	0.64%	1.24%	1.64%	1.33%	1.86%	0.97%	1.11%
Chloroflexi	Caldilineales*	0.41%	0.97%	0.48%	0.11%	0.00%	0.52%	1.80%	7.84%
Proteobacteria	Rhodospirillales*	0.39%	0.50%	0.26%	0.10%	0.11%	0.18%	0.15%	0.22%
Chloroflexi	N/A	0.32%	0.65%	0.23%	0.20%	5.95%	1.13%	0.12%	0.42%
Chloroflexi	JG30-KF-CM45*	0.23%	0.51%	0.10%	0.06%	0.00%	0.11%	0.05%	0.09%
Proteobacteria	*Sulfurifustis*	0.20%	0.39%	0.42%	0.82%	3.84%	1.37%	0.00%	0.00%
Acidobacteria	N/A	0.18%	0.35%	0.09%	0.04%	2.97%	0.18%	0.03%	0.14%
Chloroflexi	Anaerolineales*	0.17%	0.41%	0.09%	0.13%	2.67%	0.88%	0.15%	0.22%
Proteobacteria	*Reyranella*	0.16%	0.10%	0.53%	0.22%	0.00%	0.11%	6.34%	4.51%
Proteobacteria	*Mesorhizobium*	0.08%	0.20%	0.27%	0.08%	0.00%	0.01%	2.12%	1.99%
Proteobacteria	*Herminiimonas*	0.00%	0.00%	0.24%	0.22%	0.00%	0.00%	1.97%	2.81%
Bacteroidetes	*Haliscomenobacter*	0.00%	0.00%	0.04%	0.03%	0.00%	0.03%	3.05%	0.06%
Actinobacteria	*Corynebacterium*	0.00%	0.00%	0.00%	0.00%	4.08%	0.00%	0.00%	0.00%
Other	Other	20%	30%	15%	9.7%	22%	17%	22%	28%

backwashing, the relative abundance of *Legionella* in filters 1 and 2 was $0.53 \pm 0.30\%$ and $1.31 \pm 0.68\%$, respectively (Table 3). After backwashing, the relative abundance of *Legionella* in filter 1 increased to $3.01 \pm 1.66\%$ (Table 3); post-backwash samples were not collected for filter 2. Therefore, *Legionella* appear to be more difficult to remove from filters during backwashing, potentially because they are harbored by free-living amoebae. Also, the fact that the GAC rapidly quenched the free chlorine in the backwash water at DWTP2 may have exacerbated the problem. Further study is needed to determine whether the presence of *Legionella* in drinking water filters poses increased public health risks and how these potential risks (if any) can be mitigated.

3.5.2. Genus *Bradyrhizobium* in RP2

One notable observation during operation of RP2 was that ammonia concentrations increased by an average of 0.4 and 1.2 mg-N/L in the biofiltration columns receiving non-ozonated and ozonated MBR filtrate, respectively. This result contradicts other research indicating that ozone-BAC can be effective for nitrification (Chu et al., 2012). This increase in ammonia appeared to be related to backwashing frequency, which was approximately monthly at the time of media sample collection. The production of ammonia ceased following backwashing. This indicates that the bacteria responsible for ammonification accumulated during the long filter runs but were likely detached from the media during the backwash cycle.

The sequencing results indicated that *Bradyrhizobium* was the dominant genus-level OTU in all samples from RP2 prior to backwashing, with a relative abundance ranging from 19 to 61%. *Bradyrhizobium* is an aerobic, Gram negative, nitrogen-fixing soil bacterium that belongs to the phylum Proteobacteria. This is the primary reason Proteobacteria were significantly more abundant in RP2 than RP1. *Bradyrhizboium* is naturally occurring in soil and induces the formation of nodules on legume roots (Bedmar et al., 2005). Within the nodules, the bacteria can produce nitrogenase, which is an enzyme responsible for the reduction of N_2 to NH_4^+ and may explain the increase in ammonia observed in the BAC effluent. *Bradyrhizobium* is also known to generate significant quantities of EPS (Skorupska et al., 2006), which has been linked to membrane biofouling (Pang and Liu, 2007) and is consistent with the notable increase in fluorescence observed in Fig. 1. High relative abundance of *Bradyrhizobium* has not been widely reported in previous biofiltration studies, although *Rhizobium* has been reported in biofilters inoculated with activated sludge from wastewater treatment plants (Zhai et al., 2017).

Additional testing is needed to confirm that *Bradyrhizobium* was responsible for the unexpected ammonia formation and to identify the operational conditions (e.g., infrequent backwashing) responsible for its colonization of the media. Because of the potential implications of residual ammonia (e.g., free chlorine demand) and EPS release (e.g., filter clogging, DBP formation), it is important to understand how to minimize the abundance of this potential nuisance microorganism. This is comparable to preventing the proliferation of *Nocardia*, which is responsible for nuisance foam production, in activated sludge systems (Pitt and Jenkins, 1990).

4. Conclusion

The results of this study can be used as a baseline for comparing microbial community structure in other drinking water and wastewater systems. The results also highlight a number of potential linkages between microbial community structure and operational conditions in biofiltration systems that warrant further study. The most important findings are as follows:

- Biological activity within filters sometimes results in increased fluorescence associated with bulk organic matter, particularly at

Ex_{295}/Em_{410}. This is presumably due to the release of extracellular polymeric substances, which have been identified as important disinfection byproduct precursors. It is important to minimize the release of EPS to maximize total organic carbon removal in ozone-biofiltration systems and to reduce disinfection byproduct formation during final chlorination.

- The phylum Proteobacteria tends to have the highest relative abundance in drinking water treatment plants, which may be linked to the ability of some Proteobacteria to thrive in systems with low dissolved organic carbon concentrations. Proteobacteria are also abundant in wastewater treatment plants under certain operational conditions (e.g., infrequent backwashing that may select for *Bradyrhizobium*).
- The filters at some drinking water treatment plants contain a high relative abundance of the phylum Cyanobacteria, and its relative abundance increases as a function of depth. This may be due to low nitrogen levels selecting for taxa capable of nitrogen fixation and/or high ambient levels of Cyanobacteria in the source water allowing for filter colonization.
- The post-backwash media samples revealed an increase in relative abundance of endosymbionts, such as *Neochlamydia* and *Legionella*, which are known to be harbored within free-living amoebae. The lack of chlorine residual in the filter systems may have facilitated colonization by these potentially pathogenic taxa. This is a drawback of GAC biofilters, which will rapidly quench disinfectant residuals, so utilities must balance the advantages of biofiltration with the potential public health risks in various applications. Also, microbial community characterization studies targeting the 18S rRNA gene are needed to fully understand the connection between amoebae and endosymbionts in drinking water systems.
- Proteobacteria are less abundant in wastewater treatment plants with more frequent backwashing. Instead, the wastewater filters tend to be colonized by Bacteroidetes, Chloroflexi, Firmicutes, and Planctomycetes, which are commonly associated with soil, the human gut, and biological nutrient removal systems.
- Infrequent backwashing may result in the colonization of biofiltration systems by the genus *Bradyrhizobium*, which is a known ammonifier and secreter of extracellular polymeric substances. This may adversely impact potable reuse systems that target significant total organic carbon removal and employ free chlorine for final disinfection (i.e., higher disinfection byproduct formation potential).
- Microbial community structure appears to be more depth-dependent in drinking water filters than wastewater filters, potentially due to differences in redox potential and carbon/nutrient availability.
- Media type appears to cause more notable changes in beta diversity rather than alpha diversity in both drinking water and wastewater systems. Additional studies are needed to determine whether these differences in beta diversity result in the superior performance of biological activated carbon in comparison with anthracite when targeting total organic carbon removal in ozone-biofiltration systems.
- Pre-ozonation had a significant impact on alpha but not beta diversity in RP2, but this may have been an artifact of the low sample number. Greater statistical power might support the visual differences observed in the PCoAs and taxa bar plots, specifically the prevalence of *Nitrospira* in non-ozonated filters.

Acknowledgments

This publication was made possible by U.S. EPA grant R835823 (Early Career Award — Framework for Quantifying Microbial Risk and Sustainability of Potable Reuse Systems in the United States) and USGS grant G16AP00069. Its contents are solely the responsibility of the grantee and do not necessarily represent the official views of the U.S. EPA or USGS. Further, U.S. EPA and USGS do not endorse the purchase of any commercial products or services mentioned in the publication. We would also like to give special thanks to the Southern Nevada Water Authority's staff, including Edgard Verdugo and Marco Velarde for operating and maintaining the pilot and collecting media samples at RP1, and Katherine Greenstein and Julia Lew for collecting the media samples at DWTP1 and DWTP2.

Appendix A. Supplementary data

Supplementary data related to this article can be found at https://doi.org/10.1016/j.watres.2018.02.023.

References

Arnold, M., Batista, J., Dickenson, E., Gerrity, D., 2018. Use of Ozone-biofiltration for Bulk Organic Removal and Disinfection Byproduct Mitigation in Potable Reuse Applications (Submitted for publication).

Bedmar, E.J., Robles, E.F., Delgado, M.J., 2005. The complete denitrification pathway of the symbiotic, nitrogen-fixing bacterium *Bradyrhizobium japonicum*. Biochem. Soc. Trans. 33 (1), 141–144.

Bjornsson, L., Hugenholtz, P., Tyson, G.W., Blackall, L.L., 2002. Filamentous Chloroflexi (green non-sulfur bacteria) are abundant in wastewater treatment processes with biological nutrient removal. Microbiol 148, 2309–2318.

Blaha, L., Babica, P., Marsalek, B., 2009. Toxins produced in cyanobacterial water blooms—toxicity and risks. Interdiscipl. Toxicol. 2 (2), 36–41.

Caporaso, J.G., 2017. Quantitative insights into microbial ecology (QIIME) 2. https://qiime2.org. (Accessed 9 May 2017).

Caporaso, J.G., Kuczynski, J., Stombaugh, J., Bittinger, K., Bushman, F.D., Costello, E.K., Fierer, N., Pena, A.G., Goodrich, J.K., Gordon, J.I., Huttley, G.A., Kelley, S.T., Knights, D., Koenig, J.E., Ley, R.E., Lozupone, C.A., McDonald, D., Muegge, B.D., Pirrung, M., Reeder, J., Sevinsky, J.R., Turnbaugh, P.J., Walters, W.A., Widmann, J., Yatsunenko, T., Zaneveld, J., Knight, R., 2010. QIIME allows analysis of high-throughput community sequencing data. Br. J. Pharmacol. 7 (5), 335–336.

Caporaso, J.G., Lauber, C.L., Costello, E.K., Berg-Lyons, D., Gonzalez, A., Stombaugh, J., Knights, D., Gajer, P., Ravel, J., Fierer, N., Gordon, J.I., Knight, R., 2011. Moving pictures of the human microbiome. Genome Biol. 12 (5), R50.

Chandran, K., 2016. Identification of the 'active' Fraction and Metabolic Pathways in Trace Organic Compounds Removal Using Stable Isotope Probing. Water Environment Research Foundation. IWA Publishing, Alexandria, VA.

Chen, W., Westerhoff, P., Leenheer, J.A., Booksh, K., 2003. Fluorescence Excitation–Emission matrix regional integration to quantify spectra for dissolved organic matter. Environ. Sci. Technol. 37 (24), 5701–5710.

Chu, W., Gao, N., Yin, D., Deng, Y., Templeton, M.R., 2012. Ozone-biological activated carbon integrated treatment for removal of precursors of halogenated nitrogenous disinfection by-products. Chemosphere 86 (11), 1087–1091.

Daims, H., Lebedeva, E.V., Pjevac, P., Han, P., Herbold, C., Albertsen, M., Jehmlich, N., Palatinszky, M., Vierheilig, J., Bulaev, A., Kirkegaard, R.H., von Bergen, M., Rattei, T., Bendinger, B., Nielsen, P.H., Wagner, M., 2015. Complete nitrification by *Nitrospira* bacteria. Nature 528, 504–509.

de Vera, G.A., Gerrity, D., Stoker, M., Frehner, W., Wert, E.C., 2018. Microbial Activity and Community Structure in a GAC Biofilter versus Chlorinated Anthracite Filter (Submitted for publication).

Di Rienzi, S.C., Sharon, I., Wrighton, K.C., Koren, O., Hug, L.A., Thomas, B.C., Goodrich, J.K., Bell, J.T., Spector, T.D., Banfield, J.F., Ley, R.E., 2013. The human gut and groundwater harbor non-photosynthetic bacteria belonging to a new candidate phylum sibling to Cyanobacteria. eLife 2, e01102.

Douterelo, I., Boxall, J.B., Deines, P., Sekar, R., Fish, K.E., Biggs, C.A., 2014. Methodological approaches for studying the microbial ecology of drinking water distribution systems. Water Res. 65, 134–156.

Edgar, R.C., Haas, B.J., Clemente, J.C., Quince, C., Knight, R., 2011. UCHIME improves sensitivity and speed of chimera detection. Oxford J. Bioinformatics 27 (16), 2194–2200.

Eichorst, S.A., Breznak, J.A., Schmidt, T.M., 2007. Isolation and characterization of soil bacteria that define *Terriglobus* gen. nov., in the phylum *Acidobacteria*. Appl. Environ. Microbiol. 73 (8), 2708–2717.

Eiler, A., Langenheder, S., Bertilsson, S., Tranvik, L.J., 2003. Heterotrophic bacterial growth efficiency and community structure at different natural organic carbon concentrations. Appl. Environ. Microbiol. 69 (7), 3701–3709.

Fischer, K., Majewsky, M., 2014. Cometabolic degradation of organic wastewater micropollutants by activated sludge and sludge-inherent microorganisms. Appl. Microbiol. Biotechnol. 98, 6583–6597.

Fuerst, J.A., Sagulenko, E., 2011. Beyond the bacterium: Planctomycetes challenge our concepts of microbial structure and function. Nat. Rev. Microbiol. 9, 403–413.

Gerrity, D., Gamage, S., Jones, D., Korshin, G.V., Lee, Y., Pisarenko, A., Trenholm, R.A., von Gunten, U., Wert, E.C., Snyder, S.A., 2012. Development of surrogate correlation models to predict trace organic contaminant oxidation and microbial inactivation during ozonation. Water Res. 46, 6257–6272.
Hill, M.O., 1973. Diversity and evenness: a unifying notation and its consequences. Ecol 54 (2), 427–432.
Hill, T.C.J., Walsh, K.A., Harris, J.A., Moffett, B.F., 2003. Using ecological diversity measures with bacterial communities. FEMS Microbiol. Ecol. 43, 1–11.
Horn, M., Wagner, M., Muller, K., Shmid, E.N., Fritsche, T.R., Schleifer, K., Michel, R., 2000. *Neochlamydia hartmannellae* gen. nov., sp. nov. (Parachlamydiaceae), an endoparasite of the amoeba *Harmannella vermiformis*. Microbiol 146, 1231–1239.
Jałowiecki, Ł., Chojniak, J., Dorgeloh, E., Hegedusova, B., Ejhed, H., Magnér, J., Plaza, G., 2016. Microbial community profiles in wastewaters from onsite wastewater treatment systems technology. PLoS One 11 (1), e0147725.
Johnson, D.R., Helbling, D.E., Men, Y., Fenner, K., 2015. Can meta-omics help to establish causality between contaminant biotransformations and genes or gene products. Environ. Sci. Water Res. Technol 1, 272–278.
Kasuga, I., Shimazaki, D., Kunikane, S., 2007. Influence of backwashing on the microbial community in a biofilm developed on biological activated carbon used in a drinking water treatment plant. Water Sci. Technol. 55 (8–9), 173–180.
Khan, N.A., 2006. *Acanthamoeba*: biology and increasing importance in human health. FEMS Microbiol. Rev. 30, 564–595.
Kielak, A.M., Barreto, C.C., Kowalchuk, G.A., van Veen, J.A., Kuramae, E.E., 2016. The ecology of Acidobacteria: moving beyond genes and genomes. Front. Microbiol. 7, 744.
Lee, Y., Gerrity, D., Lee, M., Bogeat, A.E., Salhi, E., Gamage, S., Trenholm, R.A., Wert, E.C., Snyder, S.A., von Gunten, U., 2013. Prediction of micropollutant elimination during ozonation of municipal wastewater effluents: use of kinetic and water specific information. Environ. Sci. Technol. 47, 5872–5881.
Li, X., Upadhyaya, G., Yuen, W., Brown, J., Morgenroth, E., Raskin, L., 2010. Changes in the structure and function of microbial communities in drinking water treatment bioreactors upon addition of phosphorus. Appl. Environ. Microbiol. 76, 7473–7481.
Li, D., Sharp, J.O., Saikaly, P.E., Ali, S., Alidina, M., Alarawi, M.S., Keller, S., Hoppe-Jones, C., Drewes, J.E., 2012. Dissolved organic carbon influences microbial community composition and diversity in managed aquifer recharge systems. Appl. Environ. Microbiol. 78, 6819–6828.
Li, D., Alidina, M., Ouf, M., Sharp, J.O., Saikaly, P., Drewes, J.E., 2013. Microbial community evolution during simulated managed aquifer recharge in response to different biodegradable dissolved organic carbon (BDOC) concentrations. Water Res. 47, 2421–2430.
Li, D., Stanford, B., Dickenson, E., Khunjar, W.O., Homme, C.L., Rosenfeldt, E.J., Sharp, J.O., 2017. Effect of advanced oxidation on *N*-nitrosodimethylamine (NDMA) formation and microbial ecology during pilot-scale biological activated carbon filtration. Water Res. 13, 160–170.
Liao, X., Chen, C., Chang, C., Wang, Z., Zhang, X., Xie, S., 2012. Heterogeneity of microbial community structures inside the up-flow biological activated carbon (BAC) filters for the treatment of drinking water. Biotechnol. Bioproc. Eng. 17, 881–886.
Liao, X., Chen, C., Wang, Z., Wan, R., Chang, C., Zhang, X., Xie, S., 2013a. Changes of biomass and bacterial communities in biological activated carbon filters for drinking water treatment. Process Biochem. 48, 312–316.
Liao, X., Chen, C., Wang, Z., Wan, R., Chang, C., Zhang, X., Xie, S., 2013b. Pyrosequencing analysis of bacterial communities in drinking water biofilters receiving influents of different types. Process Biochem. 48, 703–707.
Liu, C., Olivares, C.I., Pinto, A.J., Lauderdale, C.V., Brown, J., Selbes, M., Karanfil, T., 2017. The control of disinfection byproducts and their precursors in biologically active filtration processes. Water Res. 124, 630–653.
Lucker, S., Wagner, M., Maixner, F., Pelletier, E., Koch, H., Vacherie, B., Rattei, T., Sinninghe Damste, J.S., Spieck, E., Le Paslier, D., Daims, H., 2010. A *Nitrospira* metagenome illuminates the physiology and evolution of globally important nitrite-oxidizing bacteria. Proc. Natl. Acad. Sci. U. S. A 107 (30), 13479–13484.
Mandal, S., van Treuren, W., White, R.A., Egesbo, M., Knight, R., Peddada, S.D., 2015. Analysis of composition of microbiomes: a novel method for studying microbial composition. Microb. Ecol. Health Dis. 26, 27663.
Mikkelson, K.M., Homme, C.L., Li, D., Sharp, J.O., 2015. Propane biostimulation in biologically activated carbon (BAC) selects for bacterial clades adept at degrading persistent water pollutants. Environ. Sci. Process Impacts 17, 1405–1414.
Nelson, D., LaBelle, E., 2013. *N*-nitrosodimethylamine pathway map. EAWAG. http://eawag-bbd.ethz.ch/ndm/ndm_map.html. (Accessed 9 May 2017).
Pang, C.M., Liu, W., 2007. Community structure analysis of reverse osmosis membrane biofilms and the significance of Rhizobiales bacteria in biofouling. Environ. Sci. Technol. 41 (13), 4728–4734.
Pester, M., Schleper, C., Wagner, M., 2011. The Thaumarchaeota: an emerging view of their phylogeny and ecophysiology. Curr. Opin. Microbiol. 14, 300–306.
Pitt, P., Jenkins, D., 1990. Causes and control of *Nocardia* in activated sludge. Res. J. Water Pollut. Contr. Fed. 62 (2), 143–150.
Quast, C., Pruesse, E., Yilmaz, P., Gerken, J., Schweer, T., Yarza, P., Peplies, J., Glockner, F.O., 2013. The SILVA ribosomal RNA gene database project: improved data processing and web-based tools. Nucleic Acids Res. 41, D590–D596.
Ratpukdi, T., Siripattanakul, S., Khan, E., 2010. Mineralization and biodegradability enhancement of natural organic matter by ozone-VUV in comparison with ozone, VUV, ozone-UV, and UV: effects of pH and ozone dose. Water Res. 44, 3531–3543.
Sharp, J.O., Sales, C.M., Alvarez-Cohen, L., 2010. Function characterization of propane-enhanced *N*- nitrosodimethylamine degradation by two actinomycetales. Biotechnol. Bioeng. 107 (6), 924–932.
Sinclair, L., Osman, O.A., Bertilsson, S., Eiler, A., 2015. Microbial community composition and diversity via 16S rRNA gene amplicons: evaluating the Illumina platform. PLoS One 10 (2), e011695.
Skorupska, A., Janczarek, M., Marczak, M., Mazur, A., Krol, J., 2006. Rhizobial exopolysaccharides: genetic control and symbiotic functions. Microb. Cell Factories 5 (7).
Soo, R.M., Skennerton, C.T., Sekiguchi, Y., Imelfort, M., Paech, S.J., Dennis, P.G., Steen, J.A., Parks, D.H., Tyson, G.W., Hugenholtz, P., 2014. An expanded genomic representation of the phylum Cyanobacteria. Genome Biol. Evol. 6 (5), 1031–1045.
Subramanian, S.B., Yan, S., Tyagi, R.D., Surampalli, R.Y., 2010. Extracellular polymeric substances (EPS) producing bacterial strains of municipal wastewater sludge: Isolation, molecular identification, EPS characterization and performance for sludge settling and dewatering. Water Res. 44, 2253–2266.
Thomas, F., Hehemann, J., Rebuffet, E., Czjzek, M., Michel, G., 2011. Environmental and gut Bacteroidetes: the food connection. Front. Microbiol. 2 (93).
Velten, S., Boller, M., Köster, O., Helbing, J., Weilenmann, H., Hammes, F., 2011. Development of biomass in a drinking water granular active carbon (GAC) filter. Water Res. 45 (19), 6347–6354.
Vuono, D.C., Benecke, J., Henkel, J., Navidi, W.C., Cath, T.Y., Munakata-Marr, J., Spear, J.R., Drewes, J.E., 2015. Disturbance and temporal partitioning of the activate sludge metacommunity. ISME J. 9, 425–435.
Zhai, J., Wang, Z., Shi, P., Long, C., 2017. Microbial community in a biofilter for removal of low load nitrobenzene waste gas. PLoS One 12 (1), e0170417.
Zhang, J., Kobert, K., Flouri, T., Stamatakis, A., 2013. PEAR: a fast and accurate Illumina Paired-End reAd mergeR. Bioinformatics 30 (5), 614–620.
Zhu, I.X., Getting, T., Bruce, D., 2010. Review of biologically active filters in drinking water applications. J. Am. Water Works Assoc. 102 (12), 67–77.